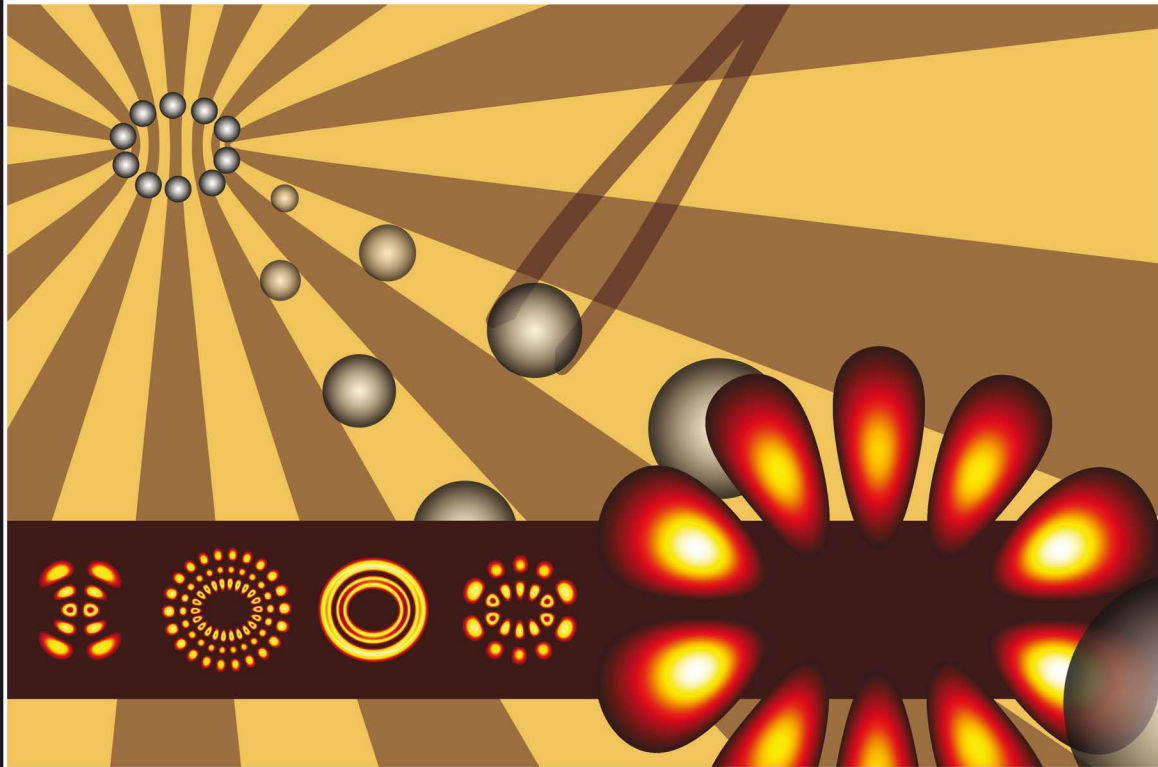


Articles published week of 14 MARCH 2011
Volume 98 Number 11

APPLIED PHYSICS LETTERS



AIP

Optical assembly of microparticles into highly ordered structures using Ince–Gaussian beams

Mike Woerdemann,^{a)} Christina Alpmann, and Cornelia Denz

Institut für Angewandte Physik, Westfälische Wilhelms-Universität Münster, Corrensstr. 2-4, 48149 Münster, Germany

(Received 18 November 2010; accepted 8 January 2011; published online 14 March 2011)

Ince–Gaussian (IG) beams are a third complete family of solutions of the paraxial Helmholtz equation. While many applications of Hermite–Gaussian and Laguerre–Gaussian beams have been demonstrated for manipulation of microparticles, the potential of the more general class of IG beams has not yet been exploited at all. We describe the unique properties of IG beams with respect to optical trapping applications, demonstrate a flexible experimental realization of arbitrary IG beams and prove the concept by creating two- and three-dimensional, highly ordered assemblies of typical microparticles. The concept is universal and can easily be integrated into existing holographic optical tweezers setups. © 2011 American Institute of Physics. [doi:10.1063/1.3561770]

During the history of optical control of matter, Hermite–Gaussian (HG) and Laguerre–Gaussian (LG) beams have been of unequalled importance. Reasons for this popularity are their availability and even more importantly their unrivaled diversity of exciting properties. The availability results directly from the fact that both families of modes are transversal eigenmodes of typical laser resonators and thus can easily be created with high efficiency.¹ Their properties include self-similarity on propagation,² a range of transversal beam profiles which can directly be transferred to complex optical potential landscapes^{3,4} and the ability of selected (LG) modes to carry and transfer optical orbital angular momentum to microscopic objects.⁵

In this letter, we introduce the more general class of Ince–Gaussian (IG) beams for applications in optical assembly and organization of matter on microscopic scales. IG beams are not only a third complete family of orthogonal solutions of the paraxial wave equation,⁶ but they also include both HG and LG beams if their ellipticity is chosen appropriately. This particular feature gives fascinating applications in optical trapping and organization as IG beams share many desired properties—like the ability to transfer optical angular momentum or the self-similarity—and at the same time exhibit new properties, including an unmatched diversity in possible optical landscapes that results from the broad range of existing transversal intensity distributions of IG beams.

In contrast to previous studies that demonstrate the generation of IG beams on a macroscopic scale,⁷ our experimental configuration utilizes focused IG beams on a microscopic scale and by this means enables advanced manipulation of microparticles. The current setup permits two modes of operation. First, three-dimensional trapping of particles in the focus region is possible. The dimension of a beam directly in the focal plane of a microscope objective typically is less than a few micrometers and the substructures of IG beams are even smaller. Hence, this mode of operation is best suited to confine particles that match or fall below the characteristic feature size of the substructure. The emphasis of this paper, however, lies on the second operation mode, the optically

guided assembly and organization of multiple particles, utilizing the particular features of IG beams.

IG beams are exact, analytical solutions of the paraxial wave equation in elliptical coordinates (η, ξ, z) , which are given by $\eta = \text{Im}\{\text{arccosh}[(x + iy)/f]\}$, $\xi = \text{Re}\{\text{arccosh}[(x + iy)/f]\}$, and $z = z$, with the semifocal separation f .^{8,9} Assuming separation of the radial and angular elliptic variables and the longitudinal variable, IG beams can be written as⁶

$$\text{IG}(\vec{r}) = E(\xi)N(\eta)\exp[iZ(z)]\Psi_G(\vec{r}), \quad (1)$$

where $\Psi_G(\vec{r})$ is the lowest order Gaussian beam. The functions $E(\xi)$ and $N(\eta)$ must obey the so called Ince equation.

The resulting transversal field distribution in any plane z can be written in terms of even (C_p^m) and odd (S_p^m) Ince polynomials of order p and degree m ,

$$\text{IG}_{p,m}^e(\vec{r}, \epsilon) = \frac{A\omega_0}{\omega(z)} C_p^m(i\xi, \epsilon) C_p^m(\eta, \epsilon) e^{i\phi(p)} \Psi_G(\vec{r}), \quad (2)$$

$$\text{IG}_{p,m}^o(\vec{r}, \epsilon) = \frac{B\omega_0}{\omega(z)} S_p^m(i\xi, \epsilon) S_p^m(\eta, \epsilon) e^{i\phi(p)} \Psi_G(\vec{r}) \quad (3)$$

with normalizing constants A, B , beam width $\omega(z)$, beam waist $\omega_0 = \omega(z=0)$, and the ellipticity parameter ϵ . The transversal intensity distribution is invariant for any plane z except for a scaling factor. Propagation is similar to the lowest order Gaussian beam with a modified Gouy phase that for IG beams is a function of the order p because of the additional phase term $\phi(p)$. The Ince polynomials are computed following a mathematical description reported elsewhere.¹⁰ Besides even and odd IG beams it is possible to construct helical IG beams (HIG) as a superposition of even and odd IG beams as follows:⁷

$$\text{HIG}_{p,m}^\pm(\vec{r}, \epsilon) = \text{IG}_{p,m}^e(\vec{r}, \epsilon) \pm i\text{IG}_{p,m}^o(\vec{r}, \epsilon). \quad (4)$$

These beams feature optical vortices,¹¹ i.e., an azimuthal inclination of the wave front, and thus carry optical orbital angular momentum similar to a subset of the LG beams (“donut modes”)¹² and helical Mathieu beams.¹³

IG beams can be generated experimentally by determining amplitude [e.g., Fig. 1(a)] and phase [Fig. 1(b)] of a light field at one plane corresponding to Eqs. (2)–(4). Since de-

^{a)}Electronic mail: woerde@uni-muenster.de.

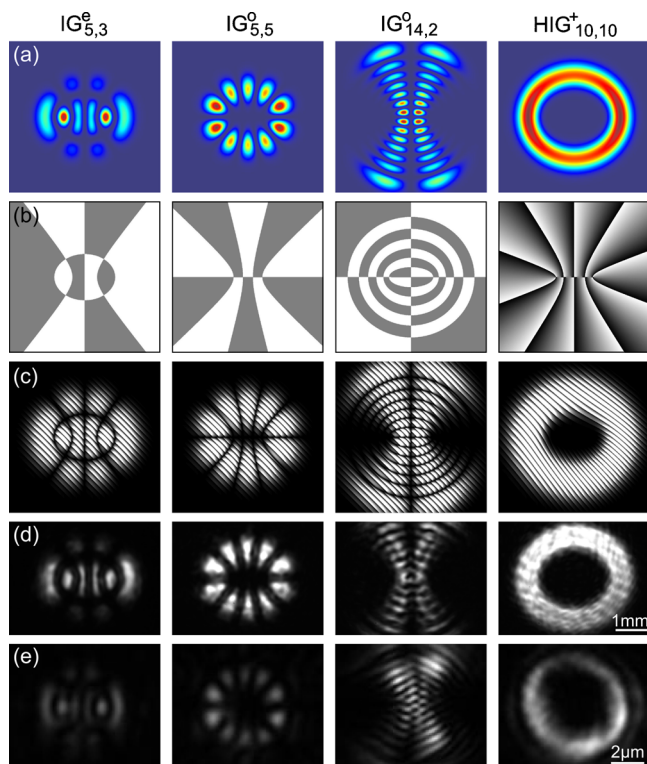


FIG. 1. (Color online) Transverse field distributions of selected IG beams. Numerical calculations of amplitude (a) and phase (b). Corresponding phase holograms with encoded amplitude information (c). Experimentally determined intensity distributions in an intermediate image plane (d) and in the focal plane of the microscope (e).

vices that can modulate the complex light field are not readily available, often phase-only spatial light modulators (PSLMs) are chosen. A phase-only filter (“phase hologram”) can additionally encode amplitude information if limitations, e.g., of the space-bandwidth product are acceptable.¹⁴ This approach enables selective and versatile generation of a wide range of different IG beams, e.g., in contrast to direct generation in laser resonators.¹⁵ A very common implementation of optical traps, holographic optical tweezers,¹⁶ also relies on PSLMs and phase holograms of IG beams can be used with existing setups with no or only slight modifications. Although this is rather a technical convenience, we believe that it might foster the fast spreading of IG beams to other laboratories, where their favorable properties for optical assembly are desired. The phase holograms for selected IG beams are depicted in Fig. 1(c).

The experimental setup (Fig. 2) that is used for optical organization of transparent microspheres with IG beams is based on a standard holographic optical tweezers setup.¹⁷ A laser beam ($P_{\max} = 2.5$ W, $\lambda = 532$ nm) is expanded and collimated such that it entirely illuminates the active area of a PSLM (Hamamatsu X8267-16, 768×768 pixels). The PSLM is imaged onto the back aperture of the microscope objective ($100\times$, $NA = 1.3$) of an inverted optical microscope. The illumination and image beam path of the microscope is kept apart from the laser beam path by means of two laser line mirrors ($\lambda = 532$ nm) that separate the blue ($\lambda \approx 470$ nm) microscope illumination from the green laser light. Located in a Fourier plane with respect to the microscope objective’s focal plane, the PSLM displays the tailored phase holograms for generation of IG beams. The IG beams

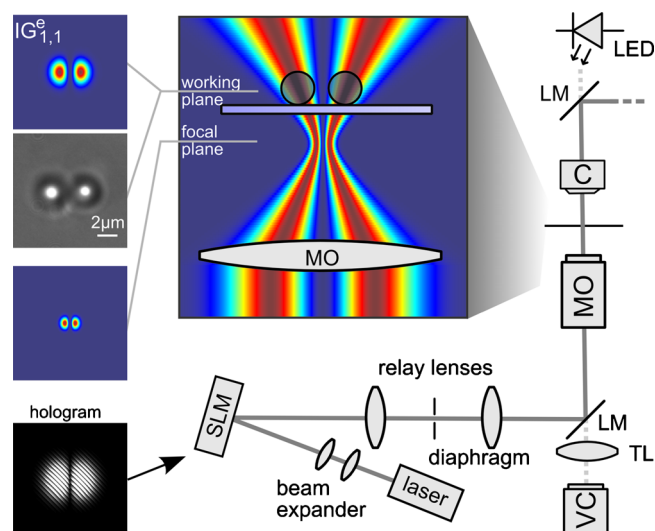


FIG. 2. (Color online) Schematic experimental setup and configuration in the vicinity of the focal plane. LM, laser line mirror; C, condenser; MO, microscope objective; TL, tube lens; VC, video camera. Insets (left column, from top) show field distribution of an $IG_{1,1}^e$ beam in the working plane, trapping of two particles, field distribution in the focal plane, and the corresponding hologram.

are generated in the first diffraction order and the zeroth order is blocked in an intermediate plane before the microscope. For this study, silica spheres with a diameter $d = 1.5$ μm , dispersed in water were used.

Figure 2 shows the configuration in the vicinity of the focal plane. The focus of an IG beam is placed slightly beneath the bottom of the sample chamber, such that the beam has already widened a little when it enters the fluid. This is important first to avoid undesired strong axial intensity gradients and second to ensure that the transversal features of the IG beams’ intensity pattern are separated sufficiently.

When the silica spheres are dispersed in the sample, they start to sediment slowly to the bottom of the sample chamber. During sedimentation they begin to feel the optical forces induced by the intensity gradients of the IG beam structure, even when the spheres are not yet close to the surface. At this point it becomes important that the shape of all IG beams is invariant during propagation. If a particle is caught in an intensity maximum at any height, it is guided along the maximum toward the focus as in an optical funnel and finally finds its position on the support. During this guided sedimentation, the optical scattering forces, which act in propagation direction of the IG beam, increase. Thus, the power of the IG beam has to be chosen adequately low, otherwise the particles are elevated and find their equilibrium position above the glass surface. For the $d = 1.5$ μm silica spheres used in our experiments, we typically used laser power of a few milliwatts, measured before the microscope objective; the actual value was adapted to the transversal extent of the respective IG beam and the distance between surface and focal plane.

Figure 3(a) shows an experimental result of organization in an $IG_{5,5}^o$ beam. Ten silica spheres occupy positions according to the ten intensity maxima of the IG beam. With structures that can accommodate more than a few particles usually not all possible positions are occupied purely by sedimentation, depending on the concentration of dispersed particles in the fluid. The fully occupied ring of ten particles

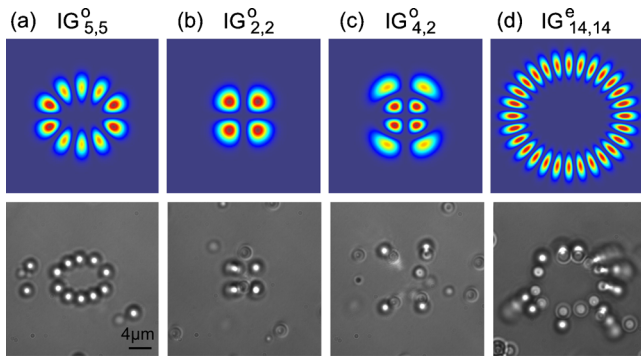


FIG. 3. (Color online) Optically assembled microstructures (bottom) and corresponding IG intensity pattern (top). (a) Ten silica spheres, organized on an $IG_{5,5}^0$ beam. [(b)–(d)] Organization and optical binding in an $IG_{2,2}^0$ beam, $IG_{4,2}^0$ beam, and $IG_{14,14}^e$ beam, respectively.

was achieved by translating the pattern of already trapped particles relative to the surface, to positions where other particles are sedimented and can be used to complete the structure.

For the assembly in Fig. 3(b), an $IG_{2,2}^0$ beam with four distinct intensity maxima was placed at a location where eight particles were sedimented close to each other. Directly after the beam is switched on, the particles organize themselves in the pattern that is imprinted by the particular IG beam. As there are more particles than intensity maxima, the surplus particles seem to pile up in the structure. This highly interesting feature of the experimental configuration can be better seen in Fig. 3(c). An $IG_{4,2}^0$ beam is used and particles are confined in the outer four intensity maxima. The inner maxima show a slightly inhomogeneous intensity distribution and are not appropriately separated to trap individual particles of the used size at each position. The outer maxima, however, do not accommodate one but two particles each, piled up in columns or chains that follow the shape of the diverging IG beam. The complete, three-dimensional structure remains intact, even when the sample chamber and thus the surface is translated relative to the structure. Most likely these chains are induced by longitudinal optical binding.¹⁸ In a simplified model of optical binding, the first sphere focuses parts of the incident light and the next particle is trapped close to this focus.¹⁹ Following this model we estimate particle–particle separations of $d_{pp} \approx 4.3 \mu\text{m}$ for plane incident wave fronts. Although we could not measure the particle–particle separations accurately, we estimate that it is close to zero and thus closer than predicted by the simple model. This can well be explained by the additional gravitational force that compresses the chains and reduces the inter-particle distances. A good approach to further investigate the binding would be the integration of a stereoscopic viewing mode.⁸

The optically bound chains can be much longer than two particles as shown in Fig. 3(d). The depicted structure is assembled by using an $IG_{14,14}^e$ beam. The structure is too small for all possible positions being occupied by particles.

Instead remaining particles form chains of four to five particles what can easily be proved by turning off the IG beam and counting the sedimenting particles. During our experiments we found even longer chains with up to ten and more bound particles each. The structures are solely hold together by optical forces; once the IG beam is turned off, the particles sediment and disperse immediately.

In summary, we proposed and demonstrated utilization of the family of IG beams for the optically guided organization of multiple microscale particles. IG beams include important properties of the well known HG and LG beams as they are a more general solution of the paraxial wave equation but feature substantially higher diversity in transversal intensity patterns and thus versatility in the range of possible optical landscapes and accessible degree of organization. The self-similarity of IG beams facilitates their generation in almost any arbitrary plane along the beam path, including the Fourier plane of the microscope objective's focal plane. It furthermore allows to choose the working plane freely in the vicinity of the focal plane, adapted to the dimensions of the envisaged colloidal structures. Besides two-dimensional organization, we achieved complex three-dimensional microstructures utilizing optical binding. The demonstrated examples might have exciting applications for coupled optical microresonator experiments with hitherto unknown complexity.

This work was partially supported by the DFG (Grant No. TRR61).

¹H. Kogelnik and T. Li, *Appl. Opt.* **5**, 1550 (1966).

²A. Forrester, M. Lonnqvist, M. J. Padgett, and J. Courtial, *Opt. Lett.* **27**, 1869 (2002).

³S. Sato, M. Ishigure, and H. Inaba, *Electron. Lett.* **27**, 1831 (1991).

⁴K. Dholakia and W. M. Lee, *Adv. At., Mol., Opt. Phys.* **56**, 261 (2008).

⁵H. He, M. E. J. Friese, N. R. Heckenberg, and H. Rubinsztein-Dunlop, *Phys. Rev. Lett.* **75**, 826 (1995).

⁶M. A. Bandres and J. C. Gutierrez-Vega, *Opt. Lett.* **29**, 144 (2004).

⁷J. Bentley, J. Davis, M. Bandres, and J. Gutierrez-Vega, *Opt. Lett.* **31**, 649 (2006).

⁸C. Alpmann, R. Bowman, M. Woerdemann, M. Padgett, and C. Denz, *Opt. Express* **18**, 26084 (2010).

⁹M. Bandres and J. Gutierrez-Vega, *J. Opt. Soc. Am. A* **21**, 873 (2004).

¹⁰F. Arscott, *Periodic Differential Equations* (Pergamon, Oxford, 1964).

¹¹L. Allen, M. W. Beijersbergen, R. J. C. Spreeuw, and J. P. Woerdman, *Phys. Rev. A* **45**, 8185 (1992).

¹²M. Woerdemann, C. Alpmann, and C. Denz, *Opt. Express* **17**, 22791 (2009).

¹³C. López-Mariscal, J. C. Gutierrez-Vega, G. Milne, and K. Dholakia, *Opt. Express* **14**, 4182 (2006).

¹⁴J. A. Davis, D. M. Cottrell, J. Campos, M. J. Yzuel, and I. Moreno, *Appl. Opt.* **38**, 5004 (1999).

¹⁵U. T. Schwarz, M. A. Bandres, and J. C. Gutierrez-Vega, *Opt. Lett.* **29**, 1870 (2004).

¹⁶E. R. Dufresne and D. G. Grier, *Rev. Sci. Instrum.* **69**, 1974 (1998).

¹⁷M. Woerdemann, S. Gläser, F. Hörner, A. Devaux, L. D. Cola, and C. Denz, *Adv. Mater.* **22**, 4176 (2010).

¹⁸S. K. Mohanty, K. S. Mohanty, and M. W. Berns, *Opt. Lett.* **33**, 2155 (2008).

¹⁹K. Dholakia and P. Zemanek, *Rev. Mod. Phys.* **82**, 1767 (2010).